Magnetic Susceptibility Tensor Anisotropies for a Lanthanide Ion Series in a Fixed Protein Matrix

Ivano Bertini,*[†,‡] Matthias B. L. Janik,[†,‡] Yong-Min Lee,[†,‡] Claudio Luchinat,[‡,§] and Antonio Rosato[†,‡]

Contribution from the Department of Chemistry, University of Florence, Via Gino Capponi 9, 50121, Florence, Italy, Centro di Risonanze Magnetiche, University of Florence, Via Luigi Sacconi 6, 50019, Sesto Fiorentino, Italy, and Department of Agricultural Biotechnology, University of Florence, P. le delle Cascine 24, 50144, Florence, Italy

Received August 2, 2000. Revised Manuscript Received January 24, 2001

Abstract: The full series of lanthanide ions (except the radioactive promethium and the S-state gadolinium) has been incorporated into the C-terminal calcium binding site of the dicalcium protein calbindin D_{9k}. A fairly constant coordination environment is maintained throughout the series. At variance with several lanthanide complexes with small chelating ligands investigated in the past, the large protein moiety provides a large number of NMR signals whose hyperfine shifts can be exclusively ascribed to pseudocontact shifts (PCS). The chemical shifts of ^{1}H and ^{15}N backbone and side chain amide NH groups were accurately measured through HSQC experiments. 1097 PCS were estimated from these by subtracting the diamagnetic contributions measured on HSQC spectra of either the $4f^0$ lanthanum(III) or the $4f^{14}$ lutetium(III) derivatives and used to define a quality factor for the structure. The differences in diamagnetic chemical shifts between the two diamagnetic blanks were relatively small, although some were not negligible especially for the nuclei closest to the metal center. These differences were used as a tolerance for the PCS. The magnetic susceptibility tensor anisotropies for each paramagnetic lanthanide ion were obtained as the result of the solution structure determination performed by using the NOEs of the cerium(III) derivative and the PCS of all lanthanides simultaneously. This set of reliable magnetic data permits an experimental assessment of Bleaney's theory relative to the magnetic properties for an extended series of lanthanide complexes in solution. All of the obtained tensors show some rhombicity, as could be expected from the lack of symmetry of the protein environment. The directions of the largest magnetic susceptibility component for Ce, Pr, Nd, Sm, Tb, Dy, and Ho and of the smallest magnetic susceptibility component for Eu, Er, Tm, and Yb were found to be all within 15° from their average (within 20° for Sm), confirming the essential similarity of the coordination environment for all lanthanides. Bleaney's theory is in excellent qualitative agreement with the observed pattern of axial anisotropies. Its quantitative agreement is substantially better than that suggested by previous analyses performed on more limited sets of PCS data for small lanthanide complexes, the so-called crystal field parameter varying only within ±30% from one lanthanide to another. These variations are even smaller (±15%) if a reasonable T^{-3} correction is taken into consideration. A knowledge of magnetic susceptibility anisotropy properties of lanthanides is essential in determining the self-orienting properties of lanthanide complexes in solution when immersed in magnetic fields.

Introduction

Pseudocontact shifts (PCS, defined as the isotropic rotational average of dipolar shifts) are observed in NMR spectra of paramagnetic molecules in solution when there is a metal-based magnetic anisotropy. They are given by[1−3]

$$\mathrm{PCS} = \delta_i^{\mathrm{pc}} = \frac{1}{12\pi r_i^3}[\Delta\chi_{\mathrm{ax}}(3\cos^2\theta - 1) + {}^3/_2\Delta\chi_{\mathrm{rh}}(\sin^2\theta\cos 2\Omega)] \quad (1)$$

where $\Delta\chi_{\mathrm{ax}}$ and $\Delta\chi_{\mathrm{rh}}$ are the axial and the rhombic anisotropies of the magnetic susceptibility tensor, and r_i, θ, and Ω are the polar coordinates of nucleus i with respect to the orthogonal reference system formed by the principal axes of the magnetic susceptibility tensor.

Equation 1 potentially contains structural information, and so has stimulated many researchers to build structural models which could be consistent with the observed PCS.[4−7] One major problem in the use of eq 1 for structural purposes has always been the definition of PCS, which is a contribution to the hyperfine shift (the other contribution being the contact shift due to unpaired electron spin delocalization). The hyperfine shift is defined as the difference between the chemical shift of a

† Department of Chemistry, University of Florence.
‡ Centro di Risonanze Magnetiche, University of Florence.
§ Department of Agricultural Biotechnology, University of Florence.

(1) McConnell, H. M.; Robertson, R. E. *J. Chem. Phys.* **1958**, *29*, 1361−1365.
(2) Kurland, R. J.; McGarvey, B. R. *J. Magn. Reson.* **1970**, *2*, 286−301.
(3) Banci, L.; Bertini, I.; Bren, K. L.; Cremonini, M. A.; Gray, H. B.; Luchinat, C.; Turano, P. *J. Biol. Inorg. Chem.* **1996**, *1*, 117−126.
(4) Barry, C. D.; North, A. C. T.; Glasel, J. A.; Williams, R. J. P.; Xavier, A. V. *Nature* **1971**, *232*, 236−245.
(5) Barry, C. D.; Glasel, J. A.; Williams, R. J. P.; Xavier, A. V. *J. Mol. Biol.* **1974**, *84*, 471−490.
(6) Barry, C. D.; Martin, D. R.; Williams, R. J. P.; Xavier, A. V. *J. Mol. Biol.* **1974**, *84*, 491−502.
(7) Gochin, M.; Roder, H. *Protein Sci.* **1995**, *4*, 296−305.

10.1021/ja0028626 CCC: $20.00
Published on Web 04/12/2001

nucleus observed in the paramagnetic compound and that of the same nucleus in a hypothetical molecule deprived of the unpaired electron(s) but with the same structure.[8−10] Even so, the definition is loose, because one or more than one unpaired electrons cannot be removed from a molecule without altering the energy of the diamagnetic core. In practice, the diamagnetic reference shift is often taken equal to the chemical shift of the same nucleus in an analogous diamagnetic compound. Then the contact shift and the PCS contributions to the hyperfine shift are separated.

It was apparent from the early work that the paramagnetic lanthanides should be superior paramagnetic probes, since the unpaired electrons are in the 4f inner shell, with the consequence that (i) the contact shift approaches zero a few covalent bonds away from the metal ion, (ii) lanthanum(III) ($4f^0$ configuration) and lutetium(III) ($4f^{14}$ configuration) are good diamagnetic analogues, and (iii) a variety of electronic structures are available (i.e. one for each lanthanide ion) with the geometric structures being essentially the same.[11−14] On this basis the literature has flourished with the aim of obtaining structural data, information on the magnetic anisotropy tensors, or, simply, better dispersion of the signals (shift reagents).[14−17] A major drawback in these applications is the presence of conformational equilibria or fluxionality around the metal ion. In this case, averaged structural data are obtained, as well as averaged magnetic anisotropy tensors. Despite these drawbacks, great advances in the theoretical understanding of these systems have been made.

Later on, proteins were found to provide ideal binding sites for the various lanthanides, as the molecular framework is relatively rigid and many nuclei can experience PCS. However, until high-field high-resolution spectrometers were available, only pioneeristic attempts at the analysis and exploitation of lanthanide-induced PCS in proteins could be made.[18−21] With the recent determination of solution structures of paramagnetic metalloproteins, further advances seem possible. In particular, PCS can be used to determine solution structures together with NOEs and other structural constraints.[3,22−26] In this approach, the solution structure is made simultaneously consistent with the experimental PCS as well as with all the other structural constraints. From this PCS-consistent solution structure, the magnetic susceptibility tensor parameters can be obtained.

Within this framework we report a determination of the magnetic susceptibility anisotropy tensors of each paramagnetic lanthanide ion bound to one of the two calcium binding sites of calbindin D_{9k}.[27] The PCS were determined for the backbone ^{15}N and amide ^{1}H nuclei, and were used to calculate the solution structure of the protein matrix and simultaneously to obtain the magnetic susceptibility anisotropy parameters. For the first time a complete set of magnetic susceptibility tensor anisotropies is available in solution which is absolutely reliable as it is not affected by the possible presence of contact contributions to the shifts and is obtained from a solution structure consistent with PCS. These results are discussed in the context of available theories and shed further light on the electronic structure of lanthanides. Furthermore, they illustrate the robustness of the PCS as structural constraints for solution structure determination of metalloproteins. Finally, the magnetic data obtained can be used as guidelines for the use of paramagnetic lanthanide ions as orienting devices in high magnetic fields.[28,29]

Materials and Methods

Sample Preparation. Protein expression[30] and purification[31] of both the Ca^{2+} and the apo form of bovine calbindin D_{9k} were performed as previously reported. The Pro43→Met43 (P43M) mutant was used to avoid any conformational heterogeneity due to *cis*−*trans* isomerization as found for the wild-type protein.[32,33] The expression system was a generous gift of Prof. S. Forsén. Uniformly ^{15}N-labeled P43M calbindin D_{9k} was obtained from M9 minimal medium containing $^{15}NH_4Cl$ as the sole nitrogen source. NMR samples were prepared by dissolving the lyophilized protein in 550 μL of either 100% D_2O or 90% H_2O/10% D_2O to final 2.0 mM protein solutions. The pH was adjusted to 6.0 by means of 0.1 M NaOH or 0.1 M HCl. Lanthanide-containing calbindin D_{9k} samples were obtained by titrating the dicalcium form with 0.02 M solutions of analytical grade $LnCl_3$ (Sigma, Aldrich) up to 1 equiv. Under these conditions, the lanthanide ions selectively substitute the calcium ion in the C-terminal site. Titrations were followed by 2D $^{1}H-^{15}N$ HSQC spectroscopy. The samples were kept at 4 °C between measurements.

NMR Spectroscopy. NMR spectra were acquired on Bruker AVANCE 800 and 400 spectrometers operating at 800.13 and 400.13 MHz, respectively. The residual water signal was suppressed by either presaturation during both the relaxation delay and mixing time or gradient-tailored excitation (WATERGATE).[34] The spectra were calibrated at different temperatures according to the empirical relationship[35] $\delta_{HOD} = (-0.012T + 5.11)$ ppm, with T being the temperature (in °C). $^{1}H-^{15}N$ HSQC[36] spectra were recorded for all lanthanide derivatives at 280, 300, and 310 K using a spectral width of 16 and 32 ppm in the ^{1}H and ^{15}N dimensions, respectively. 256 increments each with 1024 complex data points and 16 transients were collected. The recycle

(8) *NMR of Paramagnetic Molecules*; La Mar, G. N., Horrocks, W. D., Jr., Holm, R. H., Eds.; Academic Press: New York, 1973;
(9) Bertini, I.; Luchinat, C. *NMR of paramagnetic molecules in biological systems*; Benjamin/Cummings: Menlo Park, CA, 1986.
(10) Bertini, I.; Luchinat, C. *NMR of paramagnetic substances*; Coord. Chem. Rev. 150; Elsevier: Amsterdam, The Netherlands, 1996; pp 1−300.
(11) Horrocks, W. D., Jr. In *NMR of paramagnetic molecules*; La Mar, G. N., Horrocks, W. D., Jr., Holm, R. H., Eds.; Academic Press: New York, 1973; pp 479−519.
(12) Reuben, J.; Fiat, D. *J. Chem. Phys.* **1969**, *51*, 4909.
(13) Reuben, J.; Fiat, D. *Chem. Commun.* **1967**, 729.
(14) Desreux, J. F.; Fox, Z. E.; Reilley, C. N. *Anal. Chem.* **1972**, *44*, 2217.
(15) Horrocks, W. D., Jr.; Sipe, J. P., III *Science* **1972**, *177*, 994.
(16) Hinckley, C. C. *J. Am. Chem. Soc.* **1969**, *91*, 5160.
(17) Peters, J. A.; Huskens, J.; Raber, D. J. *Prog. NMR Spectrosc.* **1996**, *28*, 283−350.
(18) Campbell, I. D.; Dobson, C. M.; Williams, R. J. P.; Xavier, A. V. *Ann. N.Y. Acad. Sci.* **1973**, *222*, 163.
(19) Campbell, I. D.; Dobson, C. M.; Williams, R. J. P. *Proc. R. Soc. London* **1975**, *A345*, 41.
(20) Lee, L.; Sykes, B. D. *Biochemistry* **1980**, *19*, 3208−3214.
(21) Lee, L.; Sykes, B. D. *Biochemistry* **1983**, *22*, 4366−4373.
(22) Bentrop, D.; Bertini, I.; Cremonini, M. A.; Forsén, S.; Luchinat, C.; Malmendal, A. *Biochemistry* **1997**, *36*, 11605−11618.
(23) Banci, L.; Bertini, I.; Gray, H. B.; Luchinat, C.; Reddig, T.; Rosato, A.; Turano, P. *Biochemistry* **1997**, *36*, 9867−9877.
(24) Tu, K.; Gochin, M. *J. Am. Chem. Soc.* **1999**, *121*, 9276−9285.
(25) Allegrozzi, M.; Bertini, I.; Janik, M. B. L.; Lee, Y.-M.; Liu, G.; Luchinat, C. *J. Am. Chem. Soc.* **2000**, *122*, 4154−4161.
(26) Hus, J. C.; Marion, D.; Blackledge, M. *J. Mol. Biol.* **2000**, *298*, 927−936.
(27) Vogel, H. J.; Drakenberg, T.; Forsén, S.; O'Neil, J. D.; Hofmann, T. *Biochemistry* **1985**, *24*, 3870−3876.
(28) Tolman, J. R.; Flanagan, J. M.; Kennedy, M. A.; Prestegard, J. H. *Proc. Natl. Acad. Sci. U.S.A.* **1995**, *92*, 9279−9283.
(29) Banci, L.; Bertini, I.; Huber, J. G.; Luchinat, C.; Rosato, A. *J. Am. Chem. Soc.* **1998**, *120*, 12903−12909.
(30) Brodin, P.; Grundstrom, T.; Hofmann, T.; Drakenberg, T.; Thulin, E.; Forsén, S. *Biochemistry* **1986**, *25*, 5371−5377.
(31) Johansson, C.; Brodin, P.; Grundstrom, T.; Thulin, E.; Forsén, S.; Drakenberg, T. *Eur. J Biochem.* **1990**, *187*, 455−460.
(32) Malmendal, A.; Carlström, G.; Hambraeus, C.; Drakenberg, T.; Forsén, S.; Akke, M. *Biochemistry* **1998**, *37*, 2586−2595.
(33) Chazin, W. J.; Kördel, J.; Drakenberg, T.; Thulin, E.; Brodin, P.; Grundstrom, T.; Forsén, S. *Proc. Natl. Acad. Sci. U.S.A.* **1989**, *86*, 2195−2198.
(34) Piotto, M.; Saudek, V.; Sklenar, V. *J. Biomol. NMR* **1992**, *2*, 661−666.
(35) Bertini, I.; Ciurli, S.; Dikiy, A.; Luchinat, C. *J. Am. Chem. Soc.* **1993**, *115*, 12020−12028.
(36) Bodenhausen, G.; Ruben, D. J. *Chem. Phys. Lett.* **1980**, *69*, 185−188.

delays were in the range between 0.7 (CaTbCb) and 1.5 s (CaLaCb). For CaLaCb an additional TPPI NOESY[37,38] spectrum was recorded at 300 K with a mixing time of 100 ms, 2K data points in the f_2, and 512 increments in the f_1 dimension with 32 transients each. Raw data were multiplied in both dimensions by a squared cosine window function and Fourier transformed to obtain a final matrix of 2048 × 2048, or of 512 × 512 real data points for the HSQC spectra. A polynomial baseline correction was applied in the f_2 dimension. All NMR data were processed with the Bruker XWINNMR software packages. The program XEASY (ETH Zürich) was used for analysis of the 2D spectra.[39]

Determination of PCS and Magnetic Susceptibility Anisotropies. Pseudocontact shifts were determined by subtracting the shifts of the CaLaCb or CaLuCb protein from the particular lanthanide derivative as described in the results section. For all lanthanide derivatives, the data acquired at 300 K were used. The parameters for the magnetic susceptibility tensors for each lanthanide, $\Delta\chi_{ax}$ and $\Delta\chi_{rh}$, were obtained by simultaneously fitting all the PCS values to a family of 30 conformers obtained from solution structure calculations through eq 1. This was accomplished with the program FANTASIA.[40] The detailed procedure is reported in the following section. FANTASIA calculations were also performed on the available X-ray structure of Ca_2Cb.[41]

Structure Calculations. Resonance assignments and structural constraints other than PCS have been taken from previous work without modifications.[25] These correspond to 1539 meaningful NOEs, 6 T_1 values, and 39 ^3J values. Structure calculations were performed with a modified version of the previously described PSEUDYANA module[42] of the program DYANA.[43] The newly introduced modifications allowed all eleven sets of PCS values obtained from the various CaLnCb samples to be used in the calculations simultaneously. To do this, 11 special residues representing the magnetic susceptibility tensor of each lanthanide were added to the end of the protein sequence through linkers with null van der Waals radius, in analogy with the procedure used for calculations with a single metal ion.[23,42] The target function for PCS was defined as:

$$T^{pc} = w^{pc} \sum_{l} \sum_{i(l)} \omega_{i(l)} (|\delta^{obs}_{i(l)} - \delta^{calc}_{i(l)}| - \mathrm{tol}_{i(l)})^2 \qquad (2)$$

where w^{pc} is the weight for PCS constraints with respect to other classes of constraints (NOE, ^3J), taken equal to 1 in this work, the first summation spans all 11 lanthanides, the second summation spans all the PCS values measured for the lth lanthanide ion, $\delta^{obs}_{i(l)}$ is the ith experimental PCS value measured for the lth lanthanide, $\delta^{calc}_{i(l)}$ is the corresponding calculated value, and $\mathrm{tol}_{i(l)}$ is the corresponding tolerance. Only PCS constraints for which the absolute value of the difference between $\delta^{calc}_{i(l)}$ and $\delta^{obs}_{i(l)}$ is larger than $\mathrm{tol}_{i(l)}$ contribute to the target function.[42] The $\delta^{calc}_{i(l)}$ values are calculated at each step of the annealing procedure in PSEUDYANA through eq 1, by calculating the polar coordinates of the ith nucleus with respect to the special residue describing the lth tensor. With the present procedure, the orientation and position of each tensor is adjusted independently of those of the other tensors, and each nucleus senses simultaneously the forces due to all its available PCS constraints. An upper distance limit of 0.1 Å was introduced between the origins of the various tensors.

Two-hundred random structures were generated in PSEUDYANA calculations and annealed in 10000 steps by using the standard DYANA annealing protocol. All constraints were used simultaneously from the beginning of the annealing procedure. The axial and rhombic magnetic susceptibility anisotropies were given as input values and kept constant during the minimization. The 30 conformers with lowest target function were then used to determine again the anisotropy parameters of the magnetic susceptibility tensors with the program FANTASIA.[40] These parameters were used in a subsequent calculation as described, and the whole procedure was repeated until the parameters converged.

The Quality factor for PCS. A quality factor for PCS (Q^{pc}) has been defined in analogy with the Q factor proposed by Cornilescu et al.[44] to measure the agreement between the structure and the observed PCS values:

$$Q^{pc} = \frac{\sqrt{\sum_i (\delta^{obs}_i - \delta^{calc}_i)^2}}{\sqrt{\sum_i (\delta^{obs}_i)^2}} \qquad (3)$$

where δ^{obs}_i is the ith experimental PCS value, δ^{calc}_i is the corresponding calculated value, and the summations span all experimental PCS. The Q^{pc} factor can be calculated separately for each individual lanthanide derivative, or for all derivatives together.

Results

Preparation and Spectral Assignment of the Lanthanide Derivatives. Lanthanide-containing calbindin D_{9k} (CaLnCb) samples with a lanthanide ion replacing the calcium ion in the C-terminal site were prepared by titration of the dicalcium protein. The titration progress was followed by 2D $^1H-^{15}N$ HSQC spectroscopy. The achievement of the desired Ln^{3+}:Ca^{2+} ratio of 1:1 could be easily monitored, as cross-peaks of the Ca_2Cb form disappeared, while the new signals of the CaLnCb complex appeared. Eleven of the thirteen paramagnetic lanthanide ions were incorporated in calbindin with use of this procedure. Promethium, which is radioactive, and gadolinium, which is an S-state ion and induces extensive line broadening but vanishingly small PCS, were not considered. In all cases, only cross-peaks from a single new species were observed, showing that the lanthanide ion binds selectively at one of the two sites present in calbindin D_{9k}. The diamagnetic CaLaCb and CaLuCb derivatives were also prepared. For the latter derivatives the signal assignment of the HSQC spectra was achieved straightforwardly by visual comparison with the already assigned HSQC spectrum of the dicalcium derivative. Additionally, a 2D NOESY spectrum was recorded for CaLaCb to confirm the assignment of the signals of the residues at the metal binding site. Spectral assignments of the paramagnetic derivatives were performed following a procedure reported previously,[25] using predictions based on the metal magnetic susceptibility anisotropy. Briefly, the temperature dependence of PCS was exploited to extrapolate from the cross-peak in the paramagnetic complex to a plausible peak in the spectrum of the diamagnetic Ca_2Cb form. Based on some unambiguously assigned peaks, a magnetic susceptibility anisotropy tensor could be calculated through eq 1 (see later). With this tensor, predictions were made for the other shifted peaks, which could then be identified in the spectrum, and included in a new magnetic tensor calculation. This iterative procedure was repeated until the assignment of as many peaks as possible was obtained. Compared to the Ca_2Cb protein, not all of the theoretically observable HSQC cross-peaks could be detected in the various derivatives. The number of observable peaks depends strongly on the metal properties, as several peaks can

(37) Macura, S.; Wüthrich, K.; Ernst, R. R. *J. Magn. Reson.* **1982**, *47*, 351−357.
(38) Marion, D.; Wüthrich, K. *Biochem. Biophys. Res. Commun.* **1983**, *113*, 967−974.
(39) Eccles, C.; Güntert, P.; Billeter, M.; Wüthrich, K. *J. Biomol. NMR* **1991**, *1*, 111−130.
(40) Banci, L.; Bertini, I.; Gori Savellini, G.; Romagnoli, A.; Turano, P.; Cremonini, M. A.; Luchinat, C.; Gray, H. B. *Proteins Struct. Funct. Genet.* **1997**, *29*, 68−76.
(41) Svensson, L. A.; Thulin, E.; Forsén, S. *J. Mol. Biol.* **1992**, *223*, 601−606.
(42) Banci, L.; Bertini, I.; Cremonini, M. A.; Gori Savellini, G.; Luchinat, C.; Wüthrich, K.; Güntert, P. *J. Biomol. NMR* **1998**, *12*, 553−557.
(43) Güntert, P.; Mumenthaler, C.; Wüthrich, K. *J. Mol. Biol.* **1997**, *273*, 283−298.
(44) Cornilescu, G.; Marquardt, J.; Ottiger, M.; Bax, A. *J. Am. Chem. Soc.* **1998**, *120*, 6836−6837.

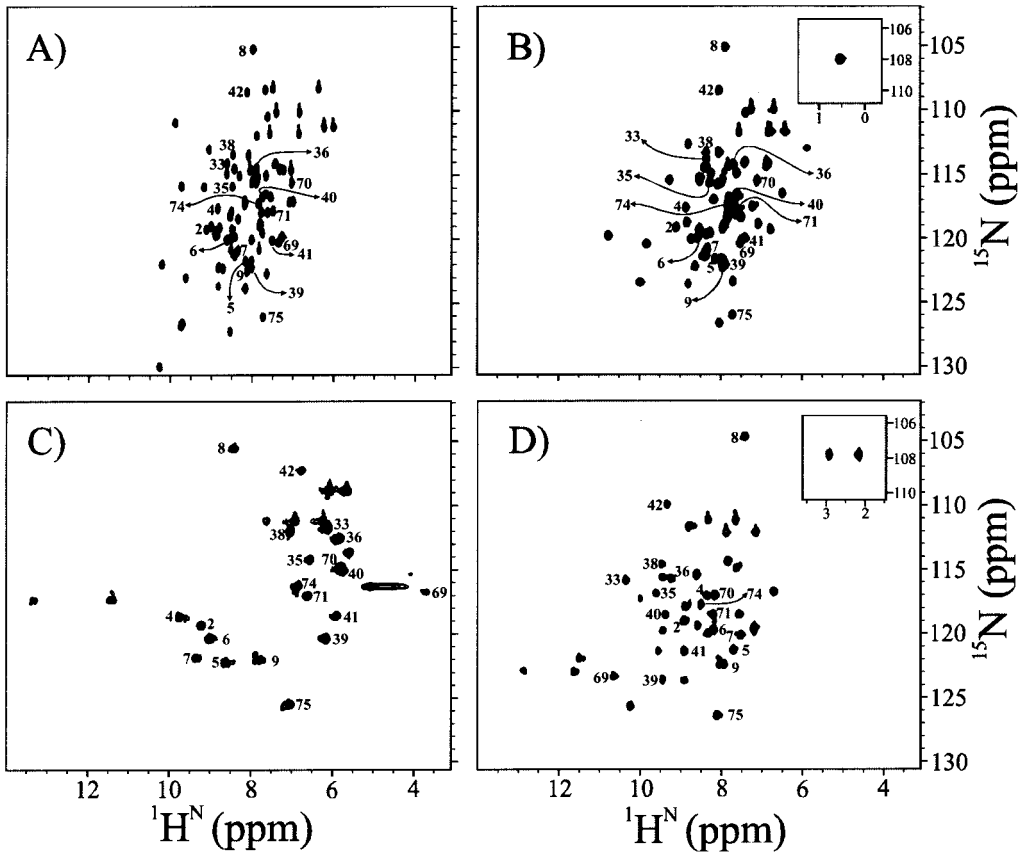

Figure 1. Representative ^{1}H−^{15}N HSQC spectra at 300 K of different CaLnCb derivatives: (A) CaLaCb; (B) CaPrCb; (C) CaTbCb; and (D) CaTmCb. Some of the peaks that (i) experience appreciable PCS in the three paramagnetic derivatives and (ii) are clearly resolved in all four spectra are labeled.

be broadened beyond detection due to paramagnetism. For CaEuCb, whose paramagnetism arises only from thermal population of excited states of the europium(III) ion, nearly all expected peaks are observed. On the other hand, in the case of CaTbCb or CaDyCb the number of observable peaks is reduced dramatically. Representative HSQC spectra are reported in Figure 1, while the assigned cross-peaks for all the metal derivatives are reported in the Supporting Information (Table S1). Some non-negligible differences in chemical shifts were observed between CaLaCb and CaLuCb, as well as differences between the shifts of either CaLaCb or CaLuCb and the Ca_2Cb derivative. The largest are found in the lanthanide binding site itself, but others are also found in the first Ca^{2+} binding site (residues 14−27), as well as in other parts of the protein (Figure 2). The differences are more pronounced on the nitrogen than on the proton shifts, as is expected since ^{15}N shifts are more sensitive to small structural changes.[45]

Determination of Pseudocontact Shifts. To achieve the highest possible reliability for the magnetic susceptibility anisotropy parameters, it is important that the uncertainty in the diamagnetic reference for each lanthanide be kept as small as possible. In any case, these uncertainties must be included in the calculations. Therefore, PCS were calculated for each paramagnetic lanthanide derivative by subtracting the shifts of either the CaLaCb or the CaLuCb complexes. These values were then fitted, for each metal, by adjusting the paramagnetic tensor parameters using the program FANTASIA [40] and by taking as an initial model the family of conformers representing the solution structure of CaCeCb determined from NOEs only. For

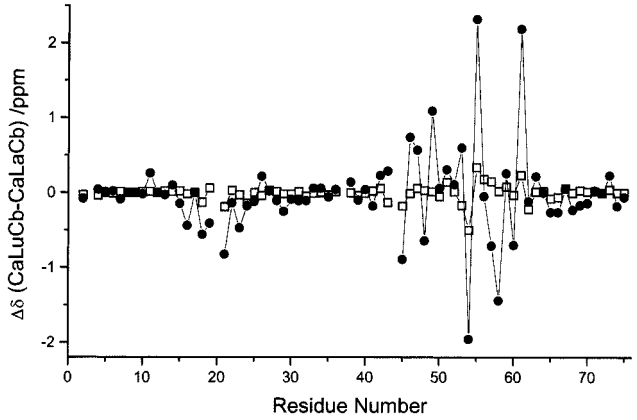

Figure 2. Differences in chemical shifts (Δδ) observed between the CaLuCb and CaLaCb derivatives for ^{1}H (open squares) and ^{15}N (filled circles) nuclei.

the early lanthanides (Ce, Pr, Nd, Sm, Eu) a better fit of the experimental data was achieved by subtracting the diamagnetic shifts of CaLaCb, whereas for the late lanthanides (Tb, Dy, Ho, Er, Tm, Yb), a better fit was obtained by subtracting the CaLuCb shifts. This observation is in agreement with expectations, as the ionic radii of lanthanides decrease along the series, so that minor alterations in the protein structure can be expected on passing from lanthanum to lutetium.[17,46,47] These alterations induce small changes in the diamagnetic shifts, which are presumably progressive along the series. To take this into

(45) Walling, A. E.; Parge, H. E.; de Dios, A. C. *J. Phys. Chem.* **1997**, *101*, 7299−7303.

(46) Peters, J. A. *J. Magn. Reson.* **1986**, *68*, 240−251.

(47) Platas, C.; Avecilla, F.; de Blas, A.; Geraldes, C. F. G. C.; Rodriguez-Blas, T.; Adams, H.; Mahia, J. *Inorg. Chem.* **1999**, *38*, 3190−3199.

account, the PCS values obtained by using the more appropriate diamagnetic reference for each paramagnetic lanthanide were assigned an uncertainty equal to the difference between the diamagnetic shifts of the CaLaCb and CaLuCb derivatives. This procedure allows the PCS constraints to accommodate possible minor structural differences which may exist between different lanthanide derivatives, particularly in the second Ca^{2+} site. The PCS of signals whose diamagnetic reference did not vary between CaLaCb and CaLuCb were assigned a small default uncertainty of 0.15 ppm. Finally, to take into account the effects of possible deviations from the point-dipole approximation of eq 1 and the possible effects of local backbone mobility on the measured PCS values, a tolerance proportional to the PCS itself was introduced (equal to 15% of the PCS value). The tolerance on each PCS used in the fittings and PSEUDYANA calculations (described below) was taken as the greater of this latter value and the uncertainty, as described above. This procedure ensures that all PCS have a minimal tolerance of 0.15 ppm. The PCS values and associated uncertainties (see Table S1) were then used to obtain the tensor parameters. PCS for the nuclei of the metal binding residues were not used in calculations.

Simultaneous Determination of Tensor Parameters and Solution Structure. The present approach for the determination of magnetic susceptibility parameters is based on the assumption that each lanthanide derivative has the same structure. This assumption is verified a posteriori by checking the agreement between the data used as input for structure calculations and their recalculated values. The full consistency between structure and PCS is reached by determining the structure with PCS as constraints. Two approaches are possible to this end: (i) a single structure is obtained by averaging the solution structures obtained from independent calculations, each using the PCS constraints of only one lanthanide derivative (together with the available NOE and ^3J values), and (ii) a unique structure calculation is performed using the PCS constraints of all lanthanides simultaneously (again, together with the NOE and ^3J values). The second procedure was chosen, and the module PSEUDYANA[42] of the DYANA program[43] has been modified for this purpose.

A total of 1097 PCS with their tolerances were used in PSEUDYANA calculations. The resulting structure has a low NOE and van der Waals target function (0.27 ± 0.05), as well as satisfactory root-mean standard deviation values from the mean structure (backbone 0.50 ± 0.13 Å, all heavy atoms 0.93 ± 0.11 Å). For the family obtained with only NOEs, the backbone RMSD value was 0.74 ± 0.19 Å, and the average total target function, which comprises NOE and van der Waals constraints, was close to 0.1. The PCS target function is around 1.7. Calculations with PCS constraints from only one or two lanthanide derivatives show that the above contribution for the PCS constraints is only marginally higher than that obtained by summing the PCS contributions from calculations on each lanthanide ion separately. In other words, the PCS contributions from the individual lanthanide derivatives to the target function are essentially additive. This implies that there are no inconsistencies between the different sets of PCS values from the individual lanthanides, suggesting that all the lanthanides bind to the same site without substantial differences in their coordination geometry. The increase in the NOE and van der Waals contribution to the target function upon introduction of the PCS constraints is modest, and the final values are well within the limits usually given for good solution structures. Importantly, no consistent violations arise upon introduction of the PCS constraints. The average Q^{pc} factor for all lanthanides for the final family is 16%. The superimposed backbone atoms of the final family of conformers are shown in Figure 3. The lanthanide ions are also displayed.

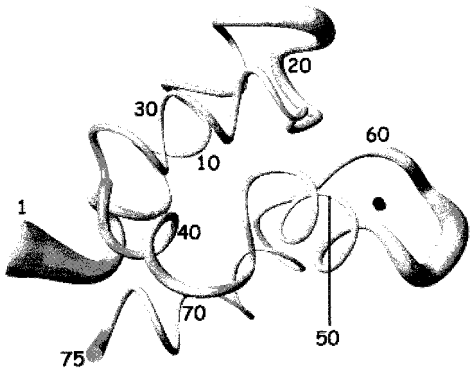

Figure 3. Display of the backbone of the final family of conformers as a tube with variable radius, proportional to the backbone RMSD of each residue. The lanthanide ions are also shown. The N- and C-terminal residues and every tenth residue are labeled. This figure was prepared with the program MOLMOL.[61]

As mentioned in the Methods section, an upper distance limit of 0.1 Å was introduced between the origins of the various tensors. This was motivated by the fact that for the most paramagnetic lanthanide ions (Dy, Tb), only a limited number of PCS were available, all relative to nuclei on the same side of the metal site and covering a relatively small solid angle. This might result in poor precision for the position of the metal ion in the binding site. If all lanthanide ions are forced to be coincident, there is no increase in the target function with respect to that obtained in the calculations which leave the position of the metal ions independent. This shows that, within the experimental uncertainty of the present data, there is no difference in the location of the lanthanide ions in the binding site. In addition, forcing the metal ions to be coincident resulted in a significant improvement of the precision of the coordinates of the family. As already mentioned, the present procedure allows the metal ions to move freely within the protein frame. At the end of the calculations, the metals appeared to be correctly positioned within the expected binding loop.

Table 1 reports the final tensor parameters as well as the angles between the principal directions of the magnetic susceptibility tensors, with the associated uncertainty. All of the derived tensors show some rhombicity, as would be expected from the lack of symmetry of the protein environment. The tensor parameters for the Dy and Yb derivatives are essentially identical with those previously reported,[25] whereas the $\Delta\chi_{ax}$ and $\Delta\chi_{rh}$ values previously determined[25] for Ce are respectively 17% and 50% lower than the present values. This is due to the different calculation procedures. In the previous paper the PCS were used to refine an existing structure, whereas now the PCS constraints (besides being more numerous because they include the PCS from 11 lanthanides) have been included from the very beginning of the calculations. Figure 4 illustrates the relative orientation of the axes of the different tensors within the protein frame. It can be seen that the magnetic susceptibility tensors of the lanthanide series have one axis pointing in the same direction (within 15° for all, and within 20° for Sm). This common direction has been taken as the *z* axis. This choice is such that the average direction of the *y* axis of the magnetic susceptibility tensor makes an angle of about 20° with the direction defined by the bond between the metal and the carbonyl oxygen of Glu60, pointing between the Cα and N atoms of Val61. The *x* axis of the same tensor instead points toward the backbone N

Table 1. Magnetic Susceptibility Tensor Parameters, $\Delta\chi_{ax}$ and $\Delta\chi_{rh}$, for the Eleven Lanthanide Derivatives of Calbindin D_{9k}

	$\Delta\chi_{ax}$ $(10^{-32}\ m^3)^a$	$\Delta\chi_{rh}$ $(10^{-32}\ m^3)^a$		x^b	y^b	z^b
CaCeCb	2.08 ± 0.13	0.71 ± 0.21	x	23 ± 15	68 ± 14	86 ± 3
			y	67 ± 15	24 ± 15	84 ± 2
			z	88 ± 3	83 ± 2	7 ± 3
CaPrCb	3.40 ± 0.18	2.11 ± 0.23	x	18 ± 4	72 ± 4	90 ± 2
			y	72 ± 4	18 ± 4	89 ± 2
			z	90 ± 2	89 ± 2	1 ± 3
CaNdCb	1.74 ± 0.09	0.46 ± 0.14	x	0 ± 13	90 ± 14	90 ± 2
			y	90 ± 14	0 ± 13	90 ± 2
			z	90 ± 2	90 ± 2	0 ± 2
CaSmCb	0.19 ± 0.04	-0.08 ± 0.05	x	45 ± 22	48 ± 16	76 ± 5
			y	44 ± 19	49 ± 27	76 ± 17
			z	89 ± 14	70 ± 11	20 ± 16
CaEuCb	-2.34 ± 0.16	-1.63 ± 0.28	x	4 ± 9	90 ± 6	86 ± 7
			y	90 ± 6	1 ± 6	89 ± 1
			z	86 ± 7	90 ± 2	5 ± 7
CaTbCb	42.1 ± 2.2	11.2 ± 1.6	x	24 ± 8	66 ± 8	85 ± 12
			y	67 ± 8	24 ± 7	85 ± 1
			z	83 ± 2	87 ± 1	8 ± 2
CaDyCb	34.7 ± 2.0	20.3 ± 1.3	x	9 ± 4	81 ± 2	88 ± 2
			y	81 ± 2	9 ± 2	89 ± 2
			z	88 ± 2	88 ± 2	3 ± 3
CaHoCb	18.5 ± 0.9	5.79 ± 1.4	x	6 ± 5	85 ± 5	86 ± 2
			y	86 ± 6	7 ± 4	85 ± 2
			z	86 ± 2	86 ± 2	6 ± 2
CaErCb	-11.6 ± 0.3	-8.58 ± 0.7	x	29 ± 6	63 ± 7	81 ± 6
			y	64 ± 7	27 ± 7	82 ± 1
			z	79 ± 3	87 ± 3	12 ± 2
CaTmCb	-21.9 ± 0.6	-20.1 ± 1.0	x	34 ± 4	56 ± 4	87 ± 1
			y	57 ± 4	34 ± 4	88 ± 1
			z	86 ± 1	90 ± 1	4 ± 2
CaYbCb	-8.26 ± 0.7	-5.84 ± 0.6	x	26 ± 6	69 ± 5	76 ± 6
			y	70 ± 5	22 ± 4	84 ± 3
			z	75 ± 7	89 ± 1	15 ± 6

[a] The $\Delta\chi$ values and axes orientations are defined according to Figure 4. The uncertainties reported correspond to the sum of the standard deviations of the tensor parameters resulting from either the fit of the individual conformers of the family or fitting partial data sets, in which 30% of the input data were randomly deleted. [b] Angles in degrees between the *x*, *y*, and *z* axes of the χ tensors for the three metals and a reference system (taken as coincident with the principal axes of the Nd(III) tensor). The uncertainties reported correspond to the sum of the standard deviations of the angles formed by the directions of the tensors resulting from either the fit of the individual conformers of the family or fitting partial data sets, in which 30% of the input data were randomly deleted.

atom of Lys55. With respect to our NMR structure available from the PDB (PDB code pending), the direction cosines of the three tensor axes in the laboratory frame are 0.895, −0.915, and −0.970 for respectively the *x*, *y*, and *z* directions. With the present choice of *z*, the sign of $\Delta\chi_{ax}$ is found to be positive for some lanthanides (Ce, Pr, Nd, Sm, Tb, Dy, and Ho) and negative for others (Eu, Er, Tm, and Yb), in complete agreement with theoretical expectations.[48] Indeed, the *z* axis as it has been defined coincides with the directions of the largest magnetic susceptibility component for Ce, Pr, Nd, Sm, Tb, Dy, and Ho and of the smallest magnetic susceptibility component for Eu, Er, Tm, and Yb. This confirms the substantial similarity of the coordination environment for all lanthanides. The present choice of the *z* axis yields $\Delta\chi_{rh} < {}^2/_3\Delta\chi_{ax}$ except for the lanthanide ions that display a negative $\Delta\chi_{ax}$. In principle, another choice of axes could have been made in order to have the *z* axis always in the direction of the largest magnetic susceptibility component for all the lanthanide ions. However, such a choice would have made comparison of the magnetic susceptibility anisotropy parameters of Table 1 physically meaningless.

The magnitude of the rhombic anisotropy and the orientation of the in-plane axes are usually affected by a higher relative error with respect to $\Delta\chi_{ax}$ and the orientation of the *z* axis, especially when $\Delta\chi_{rh}$ is small with respect to the $\Delta\chi_{ax}$ (Table 1). Thus, the $\Delta\chi_{rh}$ values will not be discussed in detail. However, it is worth pointing out that grouping the two sets of directions observed for the in-plane axes (Figure 4) as identifying the *x* and *y* axes yields signs of the $\Delta\chi_{rh}$ values that parallel those of the $\Delta\chi_{ax}$ values, except for Sm^{3+}. The latter, however, has a very low magnetic susceptibility (determined also by the contribution of excited states). In conclusion, although sometimes affected by a larger relative error, the rhombic components of the tensors also follow theoretical predictions.

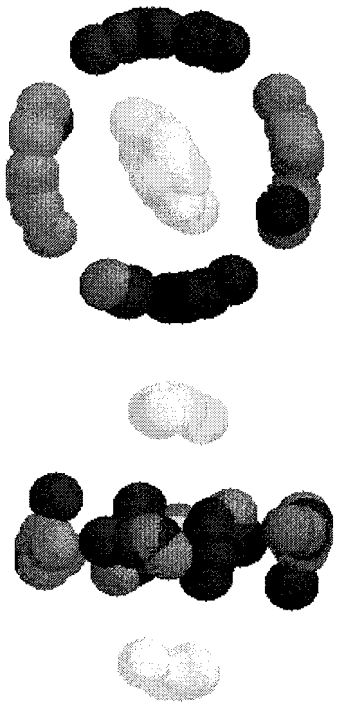

Figure 4. Display of the relative orientation within the protein frame of the magnetic susceptibility tensors of the eleven lanthanide ions studied in this work, viewed along the chosen *z* axis (top) and perpendicular to it (bottom). The spheres are centered on points along the *x* (black), *y* (dark gray), and *z* (light gray) axes, at unit distance from the origin.

Discussion

Advantages of the Calbindin D_{9k} System. The present work reports data for a homologous series of complexes in which lanthanide ions are bound to a single protein ligand. A large number of NMR signals have been detected whose hyperfine shifts may be ascribed exclusively to PCS. Despite the vast literature on the magnetic properties of lanthanide ions, very few experimental data exist on the magnetic susceptibility anisotropy along a homologous series of lanthanide complexes.[49,50] The many NMR studies addressing the issue all have been performed on relatively small ligand complexes, affording a limited number of pseudocontact-shifted signals. In addition, the shifts of some of these signals are contaminated, to various extents, by different contributions: (i) contact or ligand-centered dipolar contributions, which have been shown to be nonnegli-

(48) Bleaney, B. *J. Magn. Reson.* **1972**, *8*, 91−100.
(49) Zolin, V. F.; Koreneva, L. G. *Zh. Strukt. Khim. (Engl. Transl.)* **1980**, *21*, 51.
(50) Lisowski, J.; Sessler, J. L.; Lynch, V.; Mody, T. D. *J. Am. Chem. Soc.* **1995**, *117*, 2273−2285.
(51) Golding, R. M.; Pascual, R. O.; Vrbancich, J. *J. Mol. Phys.* **1976**, *31*, 731.

gible for nuclei separated by a few covalent bonds from the metal,[12,51] and (ii) pseudocontact contributions arising from unpaired electron spin density delocalized onto the 4f orbitals (i.e. breakdown of the point-dipole approximation) for nuclei close to the paramagnetic center.[52] Finally, relating the few reliable pseudocontact contributions to χ-tensor anisotropy parameters depends crucially on the accuracy of the atomic coordinates.[50,53] This becomes more critical the closer the nuclei of interest are to the paramagnetic center, as small atomic displacements may alter the derived tensor parameters considerably. It has been estimated that even high-resolution structural data may not be accurate enough for the purpose.[17,46] As a result of the above pitfalls, inferences on the χ-tensor anisotropy parameters along a series of lanthanide complexes are simply made, in many cases, from the shift trends observed on a very few selected signals. In these cases, the inferences can only be qualitative. The most notable exceptions are the works of Lisowski et al.[50] and Forsberg et al.,[54] which report the determination of magnetic susceptibility anisotropy values for extended series of lanthanide complexes. The average ratios between the present magnetic susceptibility anisotropy values and those reported in the above two articles are respectively 1.02 and 1.14 (excluding from the comparison the value for Tm^{3+} reported in the second work, which is clearly offset).

Theoretical Background. From the theoretical side, the origin of the magnetic anisotropy along the lanthanide series rests mainly on the treatment developed by Bleaney in the 70's.[48] In this theory, the axial and rhombic magnetic anisotropy components, $\Delta\chi_{ax}$ and $\Delta\chi_{rh}$, are proportional to the following products:

$$\Delta\chi_{ax} \propto C_J A_2^0\langle r^2\rangle \qquad \text{and} \qquad \Delta\chi_{rh} \propto C_J A_2^2\langle r^2\rangle \qquad (4)$$

where the $A_2^0\langle r^2\rangle$ and $A_2^2\langle r^2\rangle$ terms are the crystal field parameters (CFP hereafter), and $C_J \propto \langle J||\alpha||J\rangle$. The $\langle J||\alpha||J\rangle$ are numerical coefficients whose values are known for all lanthanides[48] (the C_J values for Sm^{3+} and Eu^{3+} were estimated by including the first excited states). For the sake of simplicity, the CFP are taken to be equal for all lanthanides within the homologous series.

The C_J coefficients were evaluated by assuming that the ligand field splitting of the ground-state J multiplet was negligible with respect to kT. It was shown that this is not the case.[55,56] However, the deviations from simple theory due to these higher order terms were estimated to be between 5 and 10%.[56] The order of magnitude and the sign of the correction for a number of systems have been estimated.[56] In recent years, claimed deviations of PCS patterns from Bleaney's theory have been variously attributed to (i) small structural changes along the series due to the lanthanide contraction, (ii) neglect of the splitting of the J multiplet in evaluating the C_J values, and (iii) variations of the CFP along the series.[46,47,50,57]

In view of the several sources of error that may have rendered doubtful the quantitative use of PCS in small complexes, we reiterate here the reasons why we believe the present data are quantitatively reliable: (1) Each tensor is determined by a large number of PCS values that range from 46 (for Tb^{3+}) to 132 (for Sm^{3+}). These data sets are 1 order of magnitude larger than those obtainable on small complexes. This is extremely important, as errors on PCS values and/or on atomic coordinates are random and tend to compensate each other over a large number of experimental values. (2) All the PCS values used in the present analysis originate from nuclei that are far enough from the metal center as to make contact or ligand-centered dipolar contributions negligible, and the point-dipole approximation valid. (3) As most nuclei are far from the metal, small uncertainties in their coordinates have small effects on the definition of the tensor parameters. In addition, the atomic coordinates are taken from the solution structure calculated by using the PCS of all metals simultaneously in a self-consistent procedure. The fact that the Q^{pc} factors obtained for the PCS values of each individual lanthanide when the solution structure is calculated using all lanthanides simultaneously are comparable to those obtained by performing structure calculations with the PCS of each lanthanide separately indicates that the former is equally representative of each lanthanide complex. (4) Most importantly, we believe that the modest spread of the χ-tensor axes orientations within the series is real, and arises from minor changes in the first coordination sphere on passing from one lanthanide to another. In the cases of small complexes, and therefore of a limited number of PCS, the shifts of one or more signals are followed along the series to assess the agreement with the theory. Implicitly or explicitly this procedure requires the assumption of the iso-orientation of the tensors. The present findings suggest that this may not be the case.

Comparison of Experimental Magnetic Susceptibility Data and Theoretical Expectations. The expectations from Bleaney's theory for axial systems can be confidently compared with the present experimental axial susceptibility anisotropies (as it appears from Figure 5A, open squares, the agreement is remarkable). We recall that a perfect fit would indicate (i) that the approximations in the theory introduce a negligible error and (ii) that the CFP for all lanthanides are identical, and equal to the slope of the line (172 cm^{-1}). As already discussed, estimates of CFP values for different series of lanthanide complexes have been reported.[56] Recently, variations of CFP of over a factor of 2 have been proposed in a series of lanthanide complexes on the basis of NMR data.[47,50,57] In the present case, the CFP values differ by no more than 30% from the average value of 172 cm^{-1} obtained from the fit, i.e., sizably less than expected from previous estimates. The larger variability of CFP reported for other lanthanide series could depend, at least in part, from the uncertainty of the tensor parameters, which is large when obtained for small complexes. In fact, in small complexes (i) contact shifts may be operative, which are hardly treated properly and thus the determination of PCS may be affected by errors, and (ii) the PCS are few and belong to nuclei close to the metal. When the magnetic tensor parameters are obtained, the problem arises of the detailed coincidence of the solution and solid-state structures, and of the constancy of the structure along the lanthanide series.

Higher order terms in Bleaney's theory are characterized by a T^{-3} dependence, which adds to the T^{-2} dependence that should be characteristic of lanthanide PCS.[56] The sign of these terms alternates along the series and (leaving out Sm^{3+} and Eu^{3+} that need a more complicated treatment) is positive for Ce, Nd, Tb, Ho, and Tm and negative for Pr, Dy, Er, and Yb. If Bleaney's values for the above ions are corrected by a 10% T^{-3} term, the correlation shown in Figure 5A improves further (open circles), and the variability of CFP values drops to less than 15%, which is comparable to the uncertainty on the magnetic susceptibility

(52) Golding, R. M.; Pascual, R. O.; McGarvey, B. R. *J. Magn. Reson.* **1982**, *46*, 30−30.
(53) Kemple, M. D.; Ray, B. D.; Lipkowitz, K. B.; Prendergast, F. G.; Rao, B. D. N. *J. Am. Chem. Soc.* **1988**, *110*, 8275−8287.
(54) Forsberg, J. H.; Delaney, R. M.; Zhao, Q.; Harakas, G.; Chandran, R. *Inorg. Chem.* **1995**, *34*, 3705−3715.
(55) Horrocks, W. D., Jr. *J. Magn. Reson.* **1977**, *26*, 333−339.
(56) McGarvey, B. R. *J. Magn. Reson.* **1979**, *33*, 445
(57) Ren, J.; Sherry, A. D. *J. Magn. Reson. Ser. B* **1996**, *111*, 178−182.

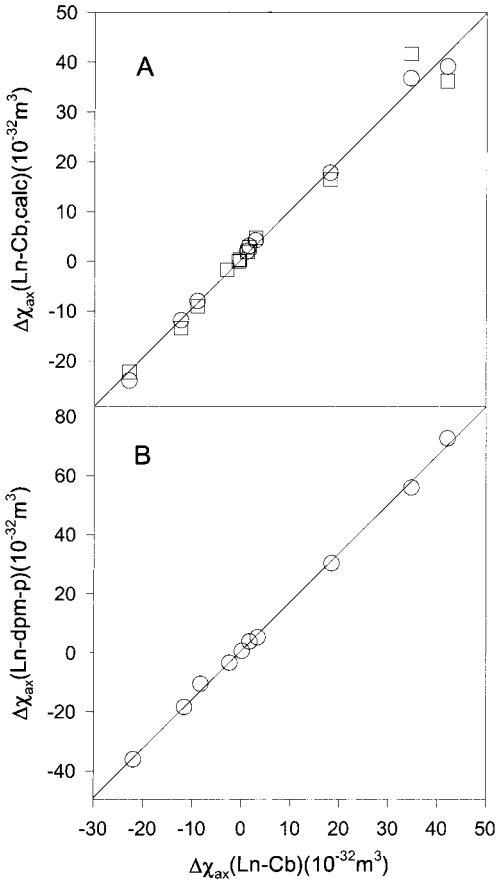

Figure 5. (A) Correlation ($r^2 = 0.976$) between experimental and calculated $\Delta\chi_{ax}$ values for the present series of lanthanides with a best fit CFP of 172 cm^{-1} (□). The same correlation ($r^2 = 0.995$) after introducing a 10% correction for the T^{-3} term with a best fit CFP of 169 cm^{-1} is also shown (○). **(**B) Correlation ($r^2 = 0.998$) between the present $\Delta\chi_{ax}$ values and experimental single-crystal values for a different series of lanthanide complexes.[15] The best fit CFP for the latter data is 282 cm^{-1}.

tensor parameters (Table 1). It can be concluded that, at least for the present series of lanthanide derivatives of calbindin D_{9k}, the variability of CFP values is much lower than what is reported in previous publications,[47,50,57] being in the range 15−30%.

Accurate magnetic susceptibility values for another, unrelated series of lanthanide complexes are available also from single-crystal measurements.[15] If the labeling of the axes reported in the original publication is scrambled for the sake of comparison with the theory and with the present data, the solid-state data are also completely consistent with our conclusions as shown in Figure 5B.

The pattern of experimental and theoretical (calculated including the above-mentioned T^{-3} correction) $\Delta\chi_{ax}$ values along the lanthanide series is shown in Figure 6. These values allow the prediction of the degree of orientation of the molecule in a high magnetic field, and, consequently, of the induced residual dipolar couplings for each lanthanide (Figure 6, right-hand scale). In a previous article, it has been shown that each protein nucleus in a lanthanide−protein complex experiences a line broadening that depends on the magnetic susceptibility of the

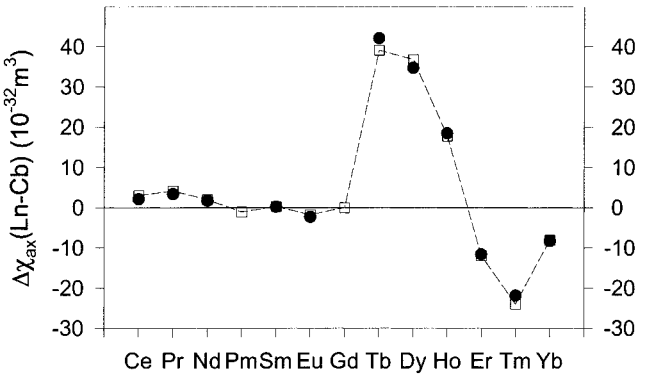

Figure 6. Experimental (filled circles) and calculated (open squares) pattern of $\Delta\chi_{ax}$ values (left-hand scale) for the present series of lanthanides. The calculated values have been obtained from eq 4 with a 10% correction for the temperature and with a CFP of 169 cm^{-1} as described in the text. The right-hand scale represents the residual dipolar coupling expected at 800 MHz and 298 K for each lanthanide. The accidental numerical coincidence of the right-hand scale (Hz) with the left-hand scale (10^{-32} m^3) is a useful mnemonic aid.

particular lanthanide. As a consequence, only nuclei that are outside a sphere of given radius (different for each lanthanide, and increasing with increasing magnetic susceptibility) can be observed.[25] With these two pieces of information at hand, one can evaluate which is the most suitable lanthanide for structural studies in terms of observability of nuclei, induced orientation-dependent effects, and dependence of the size and characteristics of the system under investigation.[58,59]

Conclusions. A reliable set of magnetic anisotropies for a full series of lanthanides is reported in this paper, and the parameters are critically evaluated with respect to the theoretical analyses available in the literature. It appears that the magnetic anisotropy values, especially the axial ones, not only closely follow the pattern predicted from theory, but also have similar values in different systems[15,50] (compare also with refs 22 and 60). The present findings allow researchers to reasonably predict the degree of orientation of the various lanthanide systems in high magnetic fields.

Acknowledgment. Thanks are expressed to Prof. Sture Forsén for providing us with the expression system for Calbindin D_{9k}. Financial support of the EU through contracts BIO4-98-0156, HPR1-1999-CT-50006, and QLG2-CT-1999-01003 is gratefully acknowledged. This work has been also partly supported by MURST, ca. 40%, and CNR (contract Nos. 97.01133.49, 98.01789.CT03, and 99.00393.49).

Supporting Information Available: Two tables reporting PCS values and tolerances used in solution structure calculations for all lanthanide derivatives (PDF). This material is available free of charge via the Internet at http://pubs.acs.org.

JA0028626

(58) Contreras, M. A.; Ubach, J.; Millet, O.; Rizo, J.; Pons, M. *J. Am. Chem. Soc.* **1999**, *121*, 8947−8948.
(59) Biekofsky, R. R.; Muskett, F. W.; Schmidt, J. M.; Martin, S. R.; Browne, J. P.; Bayley, P. M.; Feeney, J. *FEBS Lett.* **1999**, *460*, 519−526.
(60) Capozzi, F.; Cremonini, M. A.; Luchinat, C.; Sola, M. *Magn. Reson. Chem.* **1993**, *31*, S118−S127.
(61) Koradi, R.; Billeter, M.; Wüthrich, K. *J. Mol. Graphics* **1996**, *14*, 51−55.